HHS Public Access

Author manuscript

Nat Neurosci. Author manuscript; available in PMC 2017 May 21.

Published in final edited form as:

Nat Neurosci. 2017 January ; 20(1): 52–61. doi:10.1038/nn.4443.

Direct dorsal hippocampal-prelimbic cortex connections strengthen fear memories

Xiaojing Ye[1], **Dana Kapeller-Libermann**[1], **Alessio Travaglia**[1], **M. Carmen Inda**[2], and **Cristina M. Alberini**[1,3]

[1]Center for Neural Science, New York University, New York, NY, USA

Abstract

The ability to regulate the consolidation and strengthening of memories for threatening experiences is critical for mental health, and its dysregulation may lead to psychopathologies. Re-exposure to the context in which the threat was experienced can either increase or decrease fear response through distinct processes known, respectively, as reconsolidation or extinction. Using a context retrieval-dependent memory enhancement paradigm in rats, we report that memory strengthens through the activation of direct projections from the dorsal hippocampus (dHC) to the prelimbic (PL) cortex and of critical PL molecular mechanisms, which are not required for extinction. Furthermore, while a sustained PL BDNF expression is required for memory consolidation, retrieval engages PL BDNF to regulate the excitatory and inhibitory synaptic proteins neuroligin 1 and neuroligin 2, which promote memory strengthening while inhibiting extinction. Thus, context retrieval-mediated fear memory enhancement results from a concerted action of mechanisms that strengthen memory through reconsolidation while suppressing extinction.

Introduction

Memory consolidation, the process of stabilization and storage of long-term memories[1, 2], and its modulation are fundamental functions for survival. In contextual fear memories, this process engages a functional crosstalk between the dorsal hippocampus (dHC) and cortical regions[3–6]. Although hippocampal molecular mechanisms underlying long-term memory

[3]Correspondence should be addressed to: Cristina M. Alberini, Center for Neural Science, New York University, 4 Washington Place, Room 809, New York, NY, 10003, ca60@nyu.edu; Phone: 212-998-7721.

[2]Present address: Natural Sciences Department. Hostos Community College, City University of New York, Bronx, NY

Data availability

The data that support the findings of this study are available from the corresponding author upon request.

The authors claim no conflict of interest.

Author contributions

X.Y., D.K-L, A.T. M.C.I. and C.M.A. designed and developed this study. X.Y., D.K-L, A.T. and M.C.I carried out the experiments. X.Y., D.K-L, A.T. and C.M.A. wrote the manuscript.

Competing financial interests

The authors declare no competing financial interests.

consolidation have been relatively well characterized, the related cortical mechanisms remain largely unknown.

Memory consolidation can be modulated through context retrieval, the re-experience of contextual stimuli without reinforcement, to either strengthen or weaken memory retention via reconsolidation or extinction process, respectively. Reconsolidation, the process of re-stabilization of the memory after being destabilized by retrieval, mediates memory strengthening[7, 8], whereas extinction entails new learning that results in a decrease of the conditioned fear response[9, 10]. The two processes employ distinct mechanisms and can be doubly dissociated[11, 12].

Using the contextual fear-based inhibitory avoidance (IA) task in rats, we previously found that brief, non-reinforced context retrievals strengthen the memory through reconsolidation[7], which requires *de novo* translation in the basolateral amygdala (BLA)[13,14]. Recently, Fukushima *et al*.[8] reported that IA memory enhancement evoked by context retrieval in mice requires amygdala, dHC, and medial prefrontal cortex (mPFC) through the simultaneous activation of calcineurin-induced proteasome-dependent protein degradation and the transcription factor cAMP responsive element binding protein (CREB). However, important questions remain to be addressed: Why do retrieval events, in certain conditions, lead to memory enhancement rather than extinction? How do dHC and mPFC generate memory consolidation and enhancement? Are there subregions of the mPFC critically implicated in memory enhancement *vs.* extinction? Is there a functional link between reconsolidation and extinction? And, finally, which molecular, cellular and behavioral mechanisms mediate memory enhancement? The answers to these questions will elucidate circuitry and molecular mechanisms underlying fear memory strengthening or weakening, -important information for then investigating abnormal fear responses and hopefully identifying corrective approaches.

Here we employed a protocol based on three retrievals (3Rs) following IA training in rats[7], to identify hippocampal-cortical functional circuitry and mechanisms of context retrieval-induced memory strengthening. We show that 3Rs enhance fear memory by engaging direct functional connectivity between the dHC and the subregion of mPFC prelimbic (PL) cortex and two types of biological mechanisms in the PL cortex: one that promotes memory strengthening and the other that inhibits extinction.

Results

Activity-regulated cytoskeleton-associated protein (Arc/Arg3.1) in the dHC and mPFC is required for memory enhancement

Rats were trained in the IA task or remained in the homecage (non-trained, naïve group, N). Memory reactivation started 2 days (d) after training and consisted of a total of three, brief [10 seconds (s)] re-exposures to the context (the lit compartment of the IA box), given with an inter-re-exposure interval of 2 d (3Rs). Rats that were trained, but did not undergo memory reactivation (non-reactivated group, NoR), were used as controls. We also included another control group of rats, which was trained and exposed three times to a new, different context (3Cs) instead of the reactivation trials. The 3Rs protocol, given during the first week

after training, was previously proven to produce significant memory enhancement through memory reconsolidation[7].

First, we confirmed that 3Rs lead to significant memory enhancement (Fig. 1a). Western blot analyses then showed that 3Rs significantly increase the level of the activity/plasticity marker Arc/Arg3.1[15] in the dHC, BLA, mPFC and anterior cingulate cortex (ACC) 1 hour (h) after the last context retrieval, compared to both N and NoR conditions (Fig. 1b).

Compared to a control scrambled oligodeoxynucleotide (ODN), a bilateral injection of antisense ODN against Arc 1 h before each retrieval in the dHC completely blunted retrieval-mediated memory enhancement, without affecting either the memory in the absence of retrievals (NoR) or memory retrieval *per se* (Fig. 1c and Supplementary Fig. 1a). In line with previous data based on protein synthesis inhibition[8, 13], Arc antisense injection into the BLA significantly disrupted the memory (compared to scrambled ODN-injected 3Rs or NoR groups, Fig. 1c). This disruption persisted for 1 week, and memory was not rescued by a reminder shock given in a different context (Supplementary Fig. 1b), a protocol that reinstates extinguished fear memories[7], suggesting that BLA mechanisms of *de novo* gene expression, including Arc translation, mediate IA memory reconsolidation. Similarly to what was found with the dHC, Arc antisense injections into the PL or the infralimbic (IL) subregions of mPFC before each retrieval completely blocked retrieval-mediated memory enhancement without affecting the memory in the NoR groups (Fig. 1c). Finally, Arc antisense injections in the ACC had no effect on retrieval-mediated memory enhancement, indicating that not all prefrontal cortical regions are similarly engaged (Fig. 1c).

We concluded that context retrieval during the first week following IA training induces Arc expression in multiple brain regions, which is critical for processing contextual fear memories. While Arc induction in the dHC, PL and IL mediates memory enhancement, Arc induction in the BLA mediates memory reconsolidation.

Retrieval-mediated Arc induction in the dHC controls molecular mechanisms in the mPFC underlying memory enhancement

We next identified additional molecular correlates of memory enhancement in the dHC and mPFC. Western blot analyses were employed to quantify the relative activation of two mechanisms critical for long-term plasticity and memory formation: the phosphorylation of the transcription factor CREB at Ser133 (pCREB), and the phosphorylation of the actin severing protein cofilin at Ser3 (pcofilin)[16, 17]. 3Rs significantly increased both pCREB and pcofilin, but not total CREB and cofilin, in both dHC and mPFC compared to N, NoR and 3Cs (Fig. 2a and Supplementary Fig. 2). Although 3Cs did not produce memory enhancement (Fig. 1a), it significantly increased Arc in both dHC and mPFC (Fig. 2a). Furthermore, a single retrieval (1R) given at 6 d after training produced a significant increase in Arc, but only a trend toward an increase in pCREB or pcofilin in both dHC and mPFC (Fig. 2a). These data suggest that the induction of pCREB and pcofilin, but not that of Arc, correlates of memory enhancement.

Given the behavioral and molecular similarities between dHC and mPFC, we next asked whether they functionally interact to promote memory strengthening. Previous studies

suggested that hippocampal input to cortical regions is important for memory consolidation and strengthening through sleep and/or slow-wave oscillations during post-training rest periods[18]. Hence, we tested whether molecular changes evoked by 3Rs in the dHC directly control changes occurring in the mPFC. Arc antisense or scrambled control ODN was bilaterally injected into the dHC before each retrieval to block hippocampal Arc induction. Control rats received similar injections at matched time points in the absence of 3Rs (NoR). dHC and mPFC protein extracts, obtained 1 h after the last retrieval or at the matched time point for the NoR group, were examined using western blot analyses. Compared to scrambled control, Arc antisense completely blocked the 3Rs-evoked increase of Arc, pCREB and pcofilin not only in the dHC (Fig. 2b), but also –remarkably- in the mPFC (Fig. 2b). Arc antisense injections into the dHC of NoR rats did not change the levels of any of these proteins in either dHC or mPFC (Fig. 2b).

Thus, a functional crosstalk between the dHC and the mPFC underlies retrieval-mediated memory enhancement.

Direct functional dHC-PL cortex projections mediate memory enhancement

We next asked whether neuronal activity of dHC direct projections to specific subregions of the mPFC plays a critical role in memory enhancement. Within the mPFC, the IL cortex is known to mediate fear extinction, while the PL cortex plays a critical role in the expression of conditioned fear[19, 20]. Here we tested whether neuronal activity of direct projections from dHC to PL or IL cortex is involved in memory strengthening evoked by 3Rs. To verify the specificity of effects on memory strengthening, we also investigated the role of the same neuronal activation on extinction, which was evoked by confining the animals in the dark compartment of the IA box for 5 min in the absence of footshock following a standard IA test (Ext). Western blot analyses measuring Arc, pCREB and pcofilin confirmed that the dHC was activated with both 3Rs, as well as Ext given 6 days after IA training; in fact, all these markers were significantly induced with either 3Rs or extinction, compared to the N and NoR groups (Supplementary Fig. 3). Virus-mediated expression of Designer Receptors Exclusively Activated by Designer Drugs (DREADD) in the dHC projection neurons was combined with local infusion of its ligand clozapine-N-oxide (CNO) to silence neurotransmission in the PL cortex[21, 22]. Adeno-associated virus 8 (AAV8) expressing Gi-coupled DREADD hM4Di (AAV8/hSyn-HA-hM4Di-IRES-mCitrine), which in the presence of CNO silences neurotransmission[23], was injected bilaterally into the dHC. In addition to hM4Di, this viral vector also expressed a fluorescent protein mCitrine independent from HA-hM4Di in the infected neurons using the internal ribosome entry site (IRES). Unlike HA-hM4Di, which is a transmembrane protein labeling neuronal processes including long projections, mCitrine is a soluble protein and labels the somata and proximal processes of the infected cells. Four to six weeks after viral injection, infection of dHC, but not ventral hippocampal (vHC) neurons, was revealed by somatic mCitrine expression. Expression of hM4Di was detected in both the somata and neurites of infected dHC neurons, but not in the vHC (Supplementary Fig. 4a). Consistent with previous reports using a variety of retrograde tracing techniques showing a small population of dHC neurons projecting to the mPFC[24–26], in the animals injected with AAV8/hSyn-HA-hM4Di-IRES-mCitrine into the dHC, the PL cortex showed sparse hM4Di expression, indicating direct projections from the dHC to the

PL cortex (Supplementary Fig. 4b). No mCitrine-labeled neurons were detected in the PL cortex, excluding off target AAV infection. This direct projection from dHC to PL cortex was further verified and confirmed using retrograde tracer Cholera Toxin B. Injection of Cholera Toxin B into the PL cortex resulted in labeling of CA2 neurons in the rostral sections of dHC and additional sparse labeling of CA1 neurons in the caudal dHC sections (Supplementary Fig. 5a–b).

A bilateral injection of CNO into the PL cortex of rats expressing hM4Di in dHC neurons significantly reduced 3Rs-evoked Arc induction in the PL cortex, compared to control groups (vehicle injected group, or rats expressing GFP in place of hM4Di in dHC neurons and injected with CNO). No effect on Arc levels was found in the NoR group or in the IL cortex (Supplementary Fig. 5c). Compared to vehicle, CNO injection into the PL cortex completely blocked 3Rs-evoked memory enhancement. This effect persisted and did not change after a reminder shock, indicating that memory blockade was not due to a facilitated extinction, but rather to a disruption of memory strengthening (Fig. 3a). No effect of CNO injection into the PL cortex was found in the NoR group. Furthermore, injection of CNO into the PL cortex in rats expressing the control virus AAV8/hSyn-GFP in the dHC had no effect on memory retention, excluding non-specific behavioral effects caused by the virus and/or CNO (Fig. 3a).

To determine whether the dHC-PL direct projections are selectively involved in retrieval-mediated memory enhancement, we tested whether blocking the same neuronal activity had any effect on extinction. Rats bilaterally infected with AAV8/hSyn-HA-hM4Di-IRES-mCitrine in the dHC and injected with CNO in the PL cortex extinguished similarly to vehicle-injected controls (Fig. 3b). These data suggest that direct projections from dHC to PL cortex are recruited in memory strengthening, but are not involved in extinction.

Furthermore, as we found that dHC also sends direct projections to the IL cortex of mPFC (Supplementary Fig. 4b), a region known to mediate extinction, we employed the DREADD system to examine the role of neuronal activity of direct dHC to IL cortex projections in extinction. Extinction was completely blocked by a bilateral CNO injection into the IL cortex of rats whose dHC were infected with AAV8/hSyn-HA-hM4Di-IRES-mCitrine, compared to control virus AAV8/hSyn-GFP (Fig. 3b).

Collectively, these data showed that retrieval-evoked memory enhancement requires the activation of direct functional projections from the dHC to PL cortex. This activation functionally engages Arc and leads to phosphorylation of CREB and cofilin in the PL cortex. In contrast, extinction engages direct functional projections from the dHC to IL cortex.

Persistent increase in PL brain-derived neurotrophic factor (BDNF) mediates memory consolidation; retrieval engages BDNF to promote memory enhancement by inhibiting extinction

Next we investigated PL cortical mechanisms underlying retrieval-mediated memory enhancement. Given that the induction of pCREB and pcofilin correlates with memory enhancement, and that CREB-dependent gene expression as well as synaptic structural

changes accompanying synaptic plasticity and memory consolidation are regulated by BDNF[27, 28], we hypothesized that BDNF is an upstream critical mediator of memory enhancement. Western blot analyses showed that the levels of BDNF and of the phosphorylation of its receptor TrkB (pTrkB), but not total TrkB levels, were significantly increased in the mPFC 6 d after IA training compared to the N group (Fig. 4a and Supplementary Fig. 2). These upregulations were observed starting at 30 min after training and persisted for at least 1 week (Fig. 4b). Similar increases were also observed in the 3Rs group, but not in the 1R or 3Cs groups (Fig. 4a and Supplementary Fig. 2).

To block the functional role of BDNF in the PL cortex during either memory consolidation or enhancement, a functional antiBDNF blocking antibody was injected bilaterally into the PL cortex 30 min before each retrieval, or at matched time points in the absence of retrievals (NoR). Selective targeting of PL cortex injection is shown in Supplementary Fig. 6a.

Compared to IgG controls, the antiBDNF injections in the absence of retrieval significantly disrupted memory retention tested 8 d after training. The impairment persisted as shown by another test 5 days later. The memory impairment also remained after a reminder shock, suggesting that memory consolidation requires a long-lasting BDNF-dependent functional role in the PL cortex (Fig. 4c). In contrast, in the rats that underwent 3Rs, PL antiBDNF injection before each retrieval, compared to IgG, produced a distinctive outcome: it selectively blunted memory enhancement without decreasing retention below that evoked by training (Fig. 4c). This effect persisted as shown by another test 5 days later. However, a reminder shock fully rescued memory performance (Fig. 4c), indicating that the decrease in memory retention by antiBDNF reflected a facilitated extinction, rather than a disruption of memory. This effect of BDNF was different than that of other PL cortical mechanisms, such as the 3Rs-evoked Arc expression, which selectively targeted memory strengthening but did not affect extinction (Fig. 1c and Supplementary Fig. 6b). Thus, these data imply that, following context retrievals, parallel molecular mechanisms are engaged in the PL; these mechanisms, in concert, promote memory strengthening and extinction inhibition.

BDNF in the PL cortex regulates neuroligin 1 (NLGN1)/neuroligin 2 (NLGN2) ratio to promote memory consolidation or enhancement

BDNF signaling can regulate both excitatory and inhibitory synapse formation and functions[29]. Given that the balance between excitation and inhibition in the mPFC may critically contribute to fear memory expression and extinction[30, 31], we first investigated whether a change in the ratio of excitatory/inhibitory synapses accompanies 3Rs-mediated IA memory enhancement. Toward this end, we employed western blot analyses to determine whether BDNF in the PL cortex regulates the expression of NLGN1 and NLGN2, markers of maturation of excitatory and inhibitory synapses, respectively[32].

Similar to BDNF and pTrkB, both NLGN1 and NLGN2 levels in the mPFC significantly increased 6 d after IA training compared to naïve conditions (Fig. 5a), suggesting that both excitatory and inhibitory synapse maturation accompany memory consolidation. Following 1R and 3Rs, but not after 3Cs, NLGN1 level remained increased, while NLGN2 level returned to baseline after context retrieval or exposure to 3Cs (Fig. 5a). Thus, 3Rs significantly changed the ratio of NLGN1/NLGN2 (Fig. 5a) in favor of an overall

enhancement of excitatory synapse maturation, hence suggesting its functional contribution. Consistent with the conclusion that 3Rs enhance excitatory synapse maturation, GluA1 level increased after 1R and 3Rs, and GluA2 level increased after 3Rs (Supplementary Fig. 7). Hence, IA training produces a long-lasting increase in the levels of the proteins associated with both inhibitory and excitatory synapse formation and maturation in the mPFC; furthermore, context retrieval, but not exposure to a different context, increases the excitatory to inhibitory synapse ratio.

Blocking BDNF with antiBDNF antibody in the absence of retrieval blunted the training-induced increase of both NLGN1 and NLGN2 (Fig. 5b). However, blocking BDNF at each retrieval trial significantly blocked the NLGN1 induction but did not reverse the NLGN2 decrease, suggesting that the latter is mediated by BDNF-independent mechanisms (Fig. 5b). In sum, blocking BDNF significantly reversed the increased NLGN1/NLGN2 ratio after 3Rs (Fig. 5b). We concluded that BDNF signaling in the PL cortex differentially regulates inhibitory and excitatory synapse maturation after training or after context retrieval to promote memory consolidation or enhancement, respectively.

The role of NLGN1 and NLGN2 in memory consolidation, strengthening and extinction inhibition

We next examined the functional requirement for NLGN1 and NLGN2 in the PL cortex during either memory consolidation or 3Rs-evoked memory enhancement. The effect of bilateral injection into the PL cortex of the functional competitor extracellular domain of either NLGN1 or NLGN2 30 min before each retrieval, or at the matched time points in the NoR group, was tested day 8 after training. Blocking NLGN1 had no effect on memory retention in the NoR group, but completely reversed retrieval-mediated memory enhancement (Fig. 6a). This blockade persisted as shown by another test 5 days later, and the retention was not rescued by a reminder shock. Hence, functionally blocking NLGN1 produced a behavioral effect similar to that found when Arc expression was blocked (Fig. 1c and Supplementary Fig. 6b). In contrast, functional disruption of NLGN2 in the NoR group significantly and persistently disrupted memory retention tested 8 d after training, and again 5 days later. The impairment remained following a reminder shock (Fig. 6a), indicating a persistent role of PL inhibitory synapses in IA memory consolidation. On the other hand, disrupting NLGN2 function at each retrieval trial blunted memory enhancement without further disrupting the memory. The blunting effect persisted over time, but notably, a reminder shock fully rescued memory enhancement (Fig. 6a), suggesting that -like with antiBDNF- disrupting NLGN2 function promotes extinction.

To further understand the differential roles of NLGN1 and NLGN2 in memory enhancement or extinction inhibition, respectively, we investigated the activation of the PL and IL subregions of the mPFC using Arc expression as a readout[15]. A bilateral injection of NLGN1 inhibitor in the PL cortex 30 min before each retrieval trial significantly reduced Arc expression, whereas injection of NLGN2 inhibitor significantly increased Arc expression (Fig. 6b). These data confirm the knowledge that NLGN1 and NLGN2 differentially mediate excitatory and inhibitory synaptic activity[32], hence promoting or inhibiting neuronal activation, respectively. These data, in agreement with our behavioral

results, also suggest that while NLGN1 and Arc promote memory strengthening via neuronal activation (Fig. 1c, Fig. 6a and Supplementary Fig. 6b), NLGN2 inhibits neuronal activation and targets a different PL cortical mechanism that is, as indicated by our behavioral data, extinction inhibition (Fig. 6a).

To support this conclusion, we tested whether NLGN2 blockade in the PL cortex caused neuronal activation in the subregion known to mediate extinction -the IL cortex. Indeed, blocking NLGN2 in the PL cortex in the 3Rs condition increased Arc levels in both the PL and IL cortices, with the strongest effect in the IL cortex (Fig. 6b). Moreover, blocking PL NLGN1 in the 3Rs condition also led to IL cortex activation, but to a lesser degree (Fig. 6b). We concluded that NLGN1 and NLGN2 act in opposite directions in the PL cortex to functionally regulate IL cortex activation, suggesting that they likely target different neuronal populations. Together with the behavioral outcome, these data suggest that PL NLGN2 inhibits PL cortical neurons, whose function is to activate the IL cortex. Thus, this PL NLGN2-mediated inhibition ultimately suppresses extinction.

To further support this conclusion, we measured the levels of neuronal activation in an extinction paradigm. We predicted that with extinction there should be a decrease in NLGN2 in the PL cortex and more activation of the IL cortex. We therefore compared the activation of the PL and the IL cortices in the 3Rsparadigm -which as shown evokes memory enhancement (3Rs-enhancement)-, with a similar paradigm given 4 weeks after training that has previously shown to evoke IA extinction (3Rs-extinction)[7]. Neuronal activation was measured by the expression of Arc.

The number of Arc-positive cells significantly increased in the PL and the IL cortices after both enhancement and extinction paradigms; however, the increase was significantly higher in the IL cortex after 3Rs-extinction compared to 3Rs-enhancement, consistent with the previous findings that IL cortex activation is critical for memory extinction[19, 20] (Fig. 7a).

Furthermore, western blot analysis of 3Rs-enhancement and 3Rs-extinction revealed opposite directions in NLGN1 and NLGN2 expression regulation: while in the first week after training as well as with 3Rs-enhancement, NLGN1 level was significantly elevated in the mPFC (Fig. 5a), 32 d later, NLGN1 significantly decreased below the level of control N rats (Fig. 7b). NLGN2, which was increased and required for memory formation in the first week following training, decreased below control N levels 32 d later. Compared to NoR, 3Rs-extinction did not significantly change the levels of NLGN1 and NLGN2 (Fig. 7b).

BDNF and NLGN2 in the PL cortex inhibit extinction

To further dissect the PL molecular mechanisms involved in 3Rs-evoked memory enhancement *vs.* extinction, we additionally investigated the Ext paradigm. N and NoR groups served as controls. Western blot analyses revealed that the changes of Arc, pCREB, pcofilin, BDNF, pTrkB, NLGN1 and NLGN2 in the PL cortex following 3Rs are similar to those previously reported with the whole mPFC. In contrast, extinction resulted in Arc increase in the PL cortex but no change in pCREB, pcofilin, BDNF, pTrkB and NLGN1 (Supplementary Fig. 8). This suggested that extinction correlates with a very different pattern of PL cortical molecular changes.

Bilateral injections into the PL cortex of either Arc antisense, antiBDNF, or inhibitor of NLGN1 inhibitor or NLGN2 before extinction learning, (all of which as shown above blunted retrieval-mediated memory enhancement, see Fig. 1c, 4c and 6a), had no effects on memory retrieval or extinction (Fig. 8), suggesting that differential molecular mechanisms are involved in retrieval-mediated memory enhancement *vs.* extinction.

Finally, to test whether blocking PL BDNF or NLGN2 enhances extinction, as suggested by our experiments shown in Fig. 4c and 6a, we employed a weak extinction protocol. In this protocol the rats were confined to the dark compartment of the IA box for 1 min upon entering at testing. As shown in Fig. 8c and d, blocking PL BDNF or NLGN2 significantly enhanced extinction, supporting the conclusion that that these mechanisms can indeed inhibit extinction.

Collectively, these data indicate that Arc, BDNF, NLGN1 and NLGN2 in the PL cortex are specifically engaged in retrieval-mediated memory enhancement, and that BDNF and NLGN2 in the PL cortex contribute to memory enhancement by inhibiting extinction.

Discussion

The consolidation and retrieval-dependent modulation of long-term fear memories greatly influence the regulation of emotions and the development of psychopathologies. Here we provide a novel understanding of the circuitry and molecular mechanisms underlying consolidation, retrieval-dependent threat memory enhancement, and extinction.

First, we showed that IA consolidation requires several days of persistent BDNF upregulation in the PL cortex. These data significantly extend the findings that BDNF and TrkB play a critical role in the PL cortex for both appetitive and fear learning in mice[33, 34]. We also showed that PL BDNF controls the upregulation of both NLGN1 and NLGN2 in the PL cortex. To our knowledge, our data are the first to report changes of endogenous NLGN1 and NLGN2 following training in the PL cortex, and their dependence on PL BDNF. Furthermore, in line with a recent report employing a conditional NLGN2 knockout in the mPFC[35], our results reveal a critical role of NLGN2 in the PL cortex during the first week of IA memory consolidation, suggesting that the sustained inhibitory synapse function is an essential mechanism of memory consolidation. These results are important in light of the imbalance of the excitation to inhibition ratio documented in cortical areas in models of neuropsychiatry disorders[36].

Second, we showed that context retrieval following a recently formed aversive memory engages BLA for memory reconsolidation, as well as activation of a direct monosynaptic input from the dHC to the PL cortex. Fukushima *et al.*[8] have recently reported that the dHC and mPFC mediate IA memory enhancement in mice through CREB-mediated gene expression and calcineurin-induced proteasome-dependent protein degradation. Our data significantly extend this information in several ways by showing that: (i) direct functional projections from the dHC to PL cortex are necessary for memory strengthening, which occurs via Arc-dependent mechanisms in both regions. To our knowledge, this is the first evidence showing the existence of functional dHC to PL cortex direct projections in context

retrieval-mediated memory processing. (ii) The dHC activation controls PL cortical molecular mechanisms, which include the induction of pCREB, pcofilin, BDNF, pTrkB and NLGN1, to specifically promote context retrieval-induced memory enhancement. These changes are not involved in context retrieval-induced extinction. (iii) NLGN1 mediates memory strengthening. In parallel, BDNF and NLGN2 modulate memory strengthening by suppressing extinction. In agreement, we also found that, blocking BDNF or NLGN2 in the PL cortex not only did not block extinction, but actually facilitated it. These data indicate, for the first time to our knowledge, that reconsolidation and extinction are co-regulated, and are functionally cooperative processes.

Our data also showed that context retrieval shifts the role of PL BDNF-dependent mechanisms in processing hippocampal-dependent fear memory. Its functional role is required for several days after training to promote memory consolidation; however with context retrieval presentations BDNF becomes engaged in inhibiting extinction. We speculate that this shift occurs because of the activation of different memory traces that takes place with training *vs.* context retrieval. BDNF, being a common, fundamental plasticity mechanism, likely affects the active trace, therefore promoting distinct molecular and behavioral outcomes in the two behavioral paradigms (training *vs.* retrieval). Retrievals, hence memory enhancement, also resulted in the return to baseline of NLGN2 level, but not NLGN1 level, which produced a net increase in excitatory over inhibitory synapse ratio. This decrease in inhibitory synapses with retrievals was not BDNF-dependent, and can be explained by invoking a regulation of distinct populations of inhibitory synapses.

Several studies have reported that BDNF is a critical mechanism of memory extinction, which is known to mainly involve the IL cortex[37]. How can BDNF be involved in memory enhancement as well as extinction, despite these two processes being mediated by different mechanisms and circuits? We suggest that retrieval protocols and the age of the memory dictate which distinct neural circuit is activated within the dHC, BLA and mPFC neuronal subpopulations to evoke either memory strengthening through reconsolidation or extinction. We speculate that such differential regulations may involve modulation of excitatory and inhibitory connections between the PL and the IL cortices, a hypothesis in agreement with the model proposed by Miller and Cohen[38], and Baldi and Bucherelli[39]. Our speculation is also supported by our findings that memory extinction, compared to enhancement,resulted in greater activation of IL than PL cortex. Extinction also correlated with decreases in NLGN1 and NLGN2 in the mPFC, thus not changing its excitatory/inhibitory synapse ratio.

Based on our functional results targeting BDNF, NLGN1, and NLGN2 in the PL cortex, we propose, in agreement with Marquis *et al.*[40] and Ragozzino[41], that the PL cortex plays an important role in detecting and processing mismatches, thus contributing to behavioral flexibility; i.e. the first encoding of the context associated with a footshock at training is revised at retrieval by context exposure in the absence of footshock. We suggest that this mismatch is accompanied by a significant shift in the molecular regulation of plasticity through BDNF that targets the active trace. We also suggest that, in addition to the mismatch detection, other mechanisms, such as the levels of arousal and trace storage network distribution, contribute to determine when or if the memory is strengthened or extinguished.

In conclusion, the PL cortex and the input that it receives from the dHC is an important part of the circuitry that mediates and modulates the strength of hippocampal-dependent fear memory. These mechanisms may represent important targets for threat-induced psychopathologies.

Online methods

Animals

Adult male Long-Evans rats weighing 200 – 250g (age 2 – 4 months) were used for the experiments. Rats were doubly or individually housed after surgery in the New York University animal facility and maintained on a 12 h light/dark cycle with *ad libitum* access to food and water. Experiments were performed during the light cycle. All rats were handled for 3 min per day for 5 d prior to any procedure. All protocols complied with the National Institutes of Health Guide for the Care and Use of Laboratory Animals and were approved by the New York University Animal Welfare Committee.

Cannulae implants

Rats were anesthetized with ketamine (75 mg/kg) and xylazine (10 mg/kg). Stainless steel cannulae (22 gauge for dHC, 26 gauge for other brain regions) were implanted stereotactically and bilaterally to target dHC (4.0 mm posterior to Bregma, 2.6 mm lateral from midline and 2.0 mm ventral), BLA (2.8 mm posterior to Bregma, 5.3 mm lateral from midline, 6.25 mm ventral), PL (14 degree angle toward midline, 2.8 mm anterior to Bregma, 1.45 mm lateral from midline, 2.2 mm ventral), IL (30 degree angle towards midline, 2.8 mm anterior to Bregma, 3.1 mm lateral from midline, 3.3 mm ventral), ACC (26 gauge, 2.6 mm anterior to Bregma, 0.6 mm lateral from midline, 1.3 mm ventral). Rats were given buprenex (0.1 mg/kg, twice per day for 3 d pre and post-surgery) or meloxicam (3 mg/kg, once pre-surgery) for post-operational analgesic treatment, and allowed to recover for at least 8 d before training.

Inhibitory avoidance (IA)

The IA chamber (Med Associates, St. Albans, VT) consisted of a rectangular-shaped Perspex box, divided into a safe (lit) compartment and a shock (dark) compartment. Foot shocks were delivered to the grid floor of the shock compartment via a constant current scrambler circuit. The two compartments were separated by a sliding door. The chamber was located in a sound-attenuated room illuminated by dim red light. During the training session, each rat was placed in the safe compartment with its head facing away from the door. After 10 s the door was automatically opened, allowing the rat access to the shock compartment, and a 2 s 0.6 mA foot shock was administered. Latency to enter the shock compartment was taken as a measure of acquisition. 10 s after delivery of the foot shock, the rat was returned to its home cage. Memory retention was tested at the indicated time points as described in each experiment, and performed by placing the rat back into the safe compartment and measuring the latency to enter the shock compartment without administering foot shock. Testing was terminated at 900 s, and performed blind to treatments. Memory reactivation consisted of 10 s exposures to the safe compartment. In control experiments, 10 s exposures to a different context (context B, ctx B) were used. This context (control context used for the

3Cs exposures) consisted of a square chamber (Med Associates, St. Albans, VT) with three transparent walls and an opaque Plexiglas wall, and a grid with narrow spacing, located in a separate, well-lit room. To test whether memory impairment was due to extinction, animals underwent a 2 s 0.6 mA reminder foot shock in the control context. Naïve rats were handled but otherwise remained in the home cage. For memory extinction, rats were tested for memory retention in the IA box, followed by confining the animals in the dark compartment of the IA box for 5 min or 1 min (weak extinction) in the absence of foot shock, as specified.

Oligodeoxynucleotides (ODNs) and drug injections

Arc antisense (Arc AS; 5'– GTCCAGCTCCATCTGCTCGC – 3') or relative scrambled ODNs (Arc SC; 5' – CGTGCACCTCTCGCAGCTTC – 3') were dissolved in PBS pH7.4. The control Arc scrambled ODN contained the same base composition but in a randomized order, and showed no homology to any mammalian sequence in the GenBank database. The ODNs were phosphorothioated on the three terminal bases at each end to protect again nuclease degradation. The ODNs were reverse phase cartridge-purified and purchased from Gene Link (Hawthorne, NY). 2 nmol of ODNs were injected per side in the dHC (in 1 μL), PL (in 0.3 μL), IL (in 0.2 μL), BLA (in 0.5 μL) or ACC (0.5 μL), 1 h before each 10 s context reactivation trial or at the matched time points in the NoR group. The sheep functionally blocking antibody to BDNF (Millipore, Billerica, MA) or control sheep IgG (Sigma-Aldrich, St. Louis, MO) was dissolved in PBS pH7.4, and injected at 0.3 μg in 0.3 μL per injection per side into PL. Recombinant extracellular domains of NLGN1 or NLGN2 (R&D systems, Minneapolis, MN) was dissolved in PBS pH7.4, and injected at 0.12 μg in 0.3 μL per injection per side into PL. These inhibitors were injected 30 min before each 10 s context reactivation trial or at the matched time points for the NoR group. The infusion needles (28 gauge for dHC, 33 gauge for other brain regions) extended 1.5 mm beyond the cannula. Injections were carried out bilaterally with an infusion pump at a rate of 0.333 μL/min with 10 μL Hamilton syringes (for dHC, BLA and ACC) or 0.2 μL/min with 1 μL Hamilton syringes (for PL and IL). The injection needle was left in place for 2 min following the injection to allow for complete flow of the solution. For all behavioral and injection procedures, rats were randomly assigned to different groups. At the end of the behavioral experiments, the brains were collected, sectioned and examined under a light microscope to verify the cannula placement. Rats with incorrect placement were discarded from the study. In experiments that involve multiple memory retention tests, rats that lost head-caps during the course of testing were euthanized by CO2 immediately and therefore not included in the later tests.

Dissection and western blot analysis

Rats were euthanized by decapitation. Their brains were quickly dissected and sliced by a brain matrix. The brain regions of interest were dissected quickly with a scalpel in ice-cold dissection buffer. mPFC was collected from brain slices from Bregma +3.7 mm to +2.5 mm, ACC was collected from Bregma + 2.5 mm to −1.6 mm, BLA was collected from Bregma −1.6 mm to −3.6 mm, and dHC was collected from Bregma −1.6mm to −5.4 mm. The collected tissues were snap frozen on dry ice. In some experiments, PL and dHC protein extracts were generated from brains frozen in isopentane immediately following decapitation and isolated as punches in a cryostat using a neuropunch (19 gauge, Fine Science Tools,

Foster City, CA). The whole tissues collected for each brain region were homogenized in radioimmunoprecipitation assay (RIPA) buffer (150 mM NaCl, 1 % Triton X-100, 0.5 % sodium deoxycholate, 0.1 % SDS, 5 mM EDTA, 10 % glycerol, 50 mM Tris, pH8.0) supplemented with 0.5 mM PMSF, 2 mM DTT, 1 mM EGTA, 1 μM microcystin LR, 10 mM NaF, 1 mM NaOv, benzamidine, protease inhibitor cocktail and phosphatase inhibitor cocktail II and III (used as recommended by the manufacturer; Sigma, St. Louis, MO). Protein concentration was determined by the Bio-Rad protein assay (Bio-Rad Laboratories, Hercules, CA). 20 μg of total protein extract per lane were resolved using denaturing SDS-PAGE gels and transferred to Immobilon-FL membranes (Millipore, Billerica, MA) by electroblotting. Primary antibodies: rabbit anti-Arc (1:10000, Synaptic System, cat# 156 003, Gottingen, Germany), rabbit anti-pCREB (1:1000, Cell Signaling, cat# 9198, Danvers, MA), rabbit anti-pcofilin (1:3000, Abcam, cat# ab12866, Cambridge, MA), rabbit anti-BDNF (1:200, Santa Cruz Biotechnology, cat# sc-546, Santa Cruz, CA), rabbit anti-pTrkB (1:10000, Abcam, cat# 21491, Cambridge, MA), mouse anti-NLGN1 (1:1000, UC Davis/NIH NeuroMab Facility, cat# 75-160, Davis, CA; or Synaptic System, cat# 129 111, Gottingen, Germany), rabbit anti-NLGN2 (1:2000, Synaptic System, cat# 129 203, Gottingen, Germany), rabbit anti-GluA1 (1:2000, Millipore, cat# AB1504, Billerica, MA), mouse anti-GluA2 (1:1000, UC Davis/NIH NeuroMab Facility, cat# 75-002, Davis, CA), mouse anti-CREB (1:1000, Cell Signaling, cat# 9104, Danvers, MA), mouse anti-cofilin (1:2500, Abcam, cat# ab54532, Cambridge, MA) and rabbit anti-TrkB (1:1000, Cell Signaling, cat# 4603, Danvers, MA) were used. Mouse anti-actin antibody (1:20000, Santa Cruz Biotechnology, cat# sc-47778, Santa Cruz, CA) was used for loading normalization. Mouse anti-GAPDH (1:2000, Millipore, cat# MAB374, Billerica, MA) confirmed that actin did not change across experimental groups (Supplementary Fig. 9). Secondary antibodies: anti-rabbit IRDye800CW and anti-mouse IRDye680 (1:20000, Li-Cor, Lincoln, NE) were used. Membranes were scanned on the Li-Cor Odyssey imager under non-saturating conditions. Data were quantified using pixel intensities with the Odyssey software according to the protocols of the manufacturer (Li-Cor, Lincoln, NE).

Viral and clozapine-n-oxide (CNO) injections

Rats were anesthetized with ketamine (75 mg/kg) and xylazine (10 mg/kg). The skull was exposed and holes were drilled in the skull bilaterally above the dHC. A Hamilton syringe with a 28 gauge needle, mounted onto a nanopump (KD Scientific, Holliston, MA), were stereotactically inserted into the dHC (4.2 mm posterior to Bregma, 2.6 mm lateral from midline and 3.2 mm ventral). AAV8/hSyn-HA-hM4Di-IRES-mCitrine or AAV8/hSyn-GFP (2.1×10^{12} genomic copy/mL. 2 μL per side; UNC Vector Core, Chapter Hill, NC) was microinjected at a rate of 0.4 μL/min. The needle was left in place an additional 5 min following microinjection to ensure complete diffusion of the AAV, and then slowly retracted. The scalp was sutured. 3 weeks after AAV injection, the rats received stereotactic cannula implants bilaterally targeting the PL cortex, as described above. Buprenex 0.1 mg/kg) or meloxicam (3 mg/kg) was used as analgesic treatments after both surgeries, and rats were allowed to recover for 8–15 days before training. CNO (Enzo Life Sciences, Farmingdale, NY) was dissolved in PBS pH7.4, and injected at 500 μM in 0.3 μL per injection per side into PL 30 min before each 10 s context reactivation trial or at the matched time points for the NoR group, as described for the other treatments above. After behavioral experiments,

the rats were anesthetized with an i.p. injection of 750 mg/kg chloral hydrate and transcardially perfused with 4% paraformaldehyde in PBS pH7.4, and their brains were post-fixed in this solution overnight at 4°C, followed by PBS pH7.4 with 30% sucrose for 72 h. 30 μm brain sections were collected by cryosection for free-floating immunofluorescent staining. The brain sections were incubated with the blocking solution (PBS pH7.4 with 0.4% Triton X-100, 4% normal goat serum, 1% bovine serum albumin) for 1 h at room temperature. They were then stained with rabbit anti-HA antibody (1:500, Cell Signaling, cat# 3724, Danvers, MA) and chicken anti-GFP antibody (1:1000, Aves Labs, cat# GFP-1020, Tigard, OR) diluted in the blocking solution for 48 h at 4°C, followed by subsequent staining with goat anti-rabbit Alexa Fluor-568 and anti-chicken Alexa Fluor-488 antibodies (1:800, Invitrogen, Waltham, MA) for 2 h at room temperature. The sections were mounted with Prolong Diamond antifade mountant with DAPI (Invitrogen, Waltham, MA). Images were collected by the Olympus VS120 virtual slide microscope (Olympus, Tokyo, Japan) and Leica TCS SP5 confocal microscope (Leica, Wetzlar, Germany) under non-saturating conditions. Data from 19 rats were discarded due to low transduction efficiency of AAV or cannula mistargeting. Furthermore, rats that lost head-caps during the course of testing were euthanized by CO2 immediately and therefore not included in the later tests.

Cholera Toxin Subunit b (CTb) injection

Rats were anesthetized with ketamine (75 mg/kg) and xylazine (10 mg/kg). The skull was exposed and holes were drilled in the skull bilaterally above the PL. A Hamilton syringe with a 33 gauge needle, mounted onto a nanopump (KD Scientific, Holliston, MA), was stereotactically inserted into the PL (14 degree angle towards midline, 2.8 mm anterior to Bregma, 1.45 mm lateral from midline, 3.7 mm ventral). Recombinant CTb conjugated with Alexa Fluor-555 (0.5% in PBS, 0.5 μL per side; Invitrogen, Waltham, MA) was microinjected at a rate of 0.1 μL/min. The needle was left in place an additional 5 min following microinjection to ensure complete diffusion of the tracer, and then slowly retracted. The scalp was sutured. One week after injection, the rats were transcardially perfused with 4% paraformaldehyde in PBS pH7.4, and their brains were post-fixed in this solution overnight at 4°C. 40 μm brain sections were collected by a vibratome and mounted with Prolong Diamond antifade mountant with DAPI (Invitrogen, Waltham, MA). Images were collected by the Olympus VS120 virtual slide microscope (Olympus, Tokyo, Japan).

Immunofluorescent staining

Rats were anesthetized with an i.p. injection of 750 mg/kg chloral hydrate and transcardially perfused with 4% paraformaldehyde in PBS pH7.4, and their brains were post-fixed in this solution overnight at 4°C, followed by PBS pH7.4 with 30% sucrose for 72 h. 30 μm brain sections were collected by cryosection for free-floating immunofluorescent staining. For Arc staining, antigen retrieval was performed by boiling the brain sections in nanopure H_2O for 5 min. The sections were then incubated with the blocking solution (PBS pH7.4 with 0.25% Triton X-100, 4% normal goat serum, 1% bovine serum albumin) for 2 h at room temperature, followed by staining with rabbit anti-Arc antibody (1:2000, Synaptic System, cat# 156 003, Gottingen, Germany) diluted in the blocking solution for 48 h at 4°C. Subsequently, the brain sections were stained with goat anti-rabbit Alexa Fluor-568 antibody (1:800, Invitrogen, Waltham, MA) for 2 h at room temperature and mounted with Prolong

Diamond antifade mountant with DAPI (Invitrogen, Waltham, MA). Three sections around Bregma +3.2mm, +2.8mm and +2.5mm, representing rostral, medial and caudal mPFC, were used for each set of staining. Two images per side of the PL and 1 image per side of the IL cortex for each animal were captured by a Leica TCS SP5 confocal microscope (Leica, Wetzlar, Germany) at 20x. Quantification was performed using the ImageJ software (US National Institutes of Health) blinded to the experimental conditions using automated custom macro programs. Briefly, all images in an experiment were processed using the same parameters to remove background and outlier noise. Arc positive neurons were counted automatically by the Analyze Particles function using a threshold and parameters to differentiate the cytoplasmic Arc staining from the dendritic staining. The same parameters were applied to all the images. The numbers of Arc positive neurons were then normalized by the size of the region of interest.

Statistical analyses

Data were analyzed with the Prism 7 (GraphPad Software Inc.). No statistical methods were used to predetermine sample sizes, but our sample sizes are similar to those generally employed in the field. Statistical analyses were designed using the assumption of normal distribution and similar variance among groups, but this was not formally tested. The data were analyzed by one- or two-way analyses of variance (ANOVA) followed by *post hoc* tests. One-way ANOVAs followed by Newman–Keuls *post hoc* tests were performed when comparing groups for which a pairwise *post hoc* analysis of each group was required. Two-way ANOVAs followed by Bonferroni *post hoc* tests were used when two factors (such as treatment and testing) were compared. When two groups were compared, Student's *t*-tests were used. All analyses are two-tailed. The significance of the results was accepted at $P < 0.05$.

Supplementary Material

Refer to Web version on PubMed Central for supplementary material.

Acknowledgments

This work was supported by the R01-MH074736 to C.M.A, and a NARSAD Young Investigator Grant from the Brain & Behavior Research Foundation to X.Y. We thank W-J. Lin, N. Humala, G.Pollonini, K.Pandey, L.Barboza and the personnel of the animal facilities of NYU for technical support. We thank G. Philips and W-J. Lin for feedback on the manuscript.

References

1. Dudai Y. The neurobiology of consolidations, or, how stable is the engram? Annu Rev Psychol. 2004; 55:51–86. [PubMed: 14744210]
2. McGaugh JL. Memory--a century of consolidation. Science. 2000; 287:248–251. [PubMed: 10634773]
3. Squire LR, Stark CE, Clark RE. The medial temporal lobe. Annu Rev Neurosci. 2004; 27:279–306. [PubMed: 15217334]
4. Frankland PW, Bontempi B. The organization of recent and remote memories. Nat Rev Neurosci. 2005; 6:119–130. [PubMed: 15685217]
5. Kim JJ, Fanselow MS. Modality-specific retrograde amnesia of fear. Science. 1992; 256:675–677. [PubMed: 1585183]

6. Nadel L, Moscovitch M. Memory consolidation, retrograde amnesia and the hippocampal complex. Curr Opin Neurobiol. 1997; 7:217–227. [PubMed: 9142752]
7. Inda MC, Muravieva EV, Alberini CM. Memory retrieval and the passage of time: from reconsolidation and strengthening to extinction. J Neurosci. 2011; 31:1635–1643. [PubMed: 21289172]
8. Fukushima H, et al. Enhancement of fear memory by retrieval through reconsolidation. Elife. 2014; 3:e02736. [PubMed: 24963141]
9. Berman DE, Dudai Y. Memory extinction, learning anew, and learning the new: dissociations in the molecular machinery of learning in cortex. Science (New York, NY). 2001; 291:2417–2419.
10. Santini E, Ge H, Ren K, Peña de Ortiz S, Quirk GJ. Consolidation of fear extinction requires protein synthesis in the medial prefrontal cortex. The Journal of neuroscience : the official journal of the Society for Neuroscience. 2004; 24:5704–5710. [PubMed: 15215292]
11. Eisenberg M, Kobilo T, Berman DE, Dudai Y. Stability of retrieved memory: inverse correlation with trace dominance. Science. 2003; 301:1102–1104. [PubMed: 12934010]
12. Suzuki A, et al. Memory reconsolidation and extinction have distinct temporal and biochemical signatures. J Neurosci. 2004; 24:4787–4795. [PubMed: 15152039]
13. Milekic MH, Pollonini G, Alberini CM. Temporal requirement of C/EBPbeta in the amygdala following reactivation but not acquisition of inhibitory avoidance. Learn Mem. 2007; 14:504–511. [PubMed: 17644752]
14. Alberini CM. Mechanisms of memory stabilization: are consolidation and reconsolidation similar or distinct processes? Trends Neurosci. 2005; 28:51–56. [PubMed: 15626497]
15. Korb E, Finkbeiner S. Arc in synaptic plasticity: from gene to behavior. Trends Neurosci. 2011; 34:591–598. [PubMed: 21963089]
16. Alberini CM. Transcription factors in long-term memory and synaptic plasticity. Physiol Rev. 2009; 89:121–145. [PubMed: 19126756]
17. Gu J, et al. ADF/cofilin-mediated actin dynamics regulate AMPA receptor trafficking during synaptic plasticity. Nat Neurosci. 2010; 13:1208–1215. [PubMed: 20835250]
18. Schwindel CD, McNaughton BL. Hippocampal-cortical interactions and the dynamics of memory trace reactivation. Prog Brain Res. 2011; 193:163–177. [PubMed: 21854962]
19. Sierra-Mercado D, Padilla-Coreano N, Quirk GJ. Dissociable roles of prelimbic and infralimbic cortices, ventral hippocampus, and basolateral amygdala in the expression and extinction of conditioned fear. Neuropsychopharmacology. 2011; 36:529–538. [PubMed: 20962768]
20. Sotres-Bayon F, Quirk GJ. Prefrontal control of fear: more than just extinction. Curr Opin Neurobiol. 2010; 20:231–235. [PubMed: 20303254]
21. Urban DJ, Roth BL. DREADDs (designer receptors exclusively activated by designer drugs): chemogenetic tools with therapeutic utility. Annu Rev Pharmacol Toxicol. 2015; 55:399–417. [PubMed: 25292433]
22. Stachniak TJ, Ghosh A, Sternson SM. Chemogenetic synaptic silencing of neural circuits localizes a hypothalamus-->midbrain pathway for feeding behavior. Neuron. 2014; 82:797–808. [PubMed: 24768300]
23. Armbruster BN, Li X, Pausch MH, Herlitze S, Roth BL. Evolving the lock to fit the key to create a family of G protein-coupled receptors potently activated by an inert ligand. Proc Natl Acad Sci U S A. 2007; 104:5163–5168. [PubMed: 17360345]
24. Hoover WB, Vertes RP. Anatomical analysis of afferent projections to the medial prefrontal cortex in the rat. Brain Struct Funct. 2007; 212:149–179. [PubMed: 17717690]
25. Xu W, Sudhof TC. A neural circuit for memory specificity and generalization. Science. 2013; 339:1290–1295. [PubMed: 23493706]
26. DeNardo LA, Berns DS, DeLoach K, Luo L. Connectivity of mouse somatosensory and prefrontal cortex examined with trans-synaptic tracing. Nat Neurosci. 2015; 18:1687–1697. [PubMed: 26457553]
27. Bambah-Mukku D, Travaglia A, Chen DY, Pollonini G, Alberini CM. A positive autoregulatory BDNF feedback loop via C/EBPbeta mediates hippocampal memory consolidation. J Neurosci. 2014; 34:12547–12559. [PubMed: 25209292]

28. Rex CS, et al. Brain-derived neurotrophic factor promotes long-term potentiation-related cytoskeletal changes in adult hippocampus. J Neurosci. 2007; 27:3017–3029. [PubMed: 17360925]
29. Gottmann K, Mittmann T, Lessmann V. BDNF signaling in the formation, maturation and plasticity of glutamatergic and GABAergic synapses. Exp Brain Res. 2009; 199:203–234. [PubMed: 19777221]
30. Riga D, et al. Optogenetic dissection of medial prefrontal cortex circuitry. Front Syst Neurosci. 2014; 8:230. [PubMed: 25538574]
31. Courtin J, et al. Prefrontal parvalbumin interneurons shape neuronal activity to drive fear expression. Nature. 2014; 505:92–96. [PubMed: 24256726]
32. Sudhof TC. Neuroligins and neurexins link synaptic function to cognitive disease. Nature. 2008; 455:903–911. [PubMed: 18923512]
33. Choi DC, Gourley SL, Ressler KJ. Prelimbic BDNF and TrkB signaling regulates consolidation of both appetitive and aversive emotional learning. Transl Psychiatry. 2012; 2:e205. [PubMed: 23250006]
34. Choi DC, et al. Prelimbic cortical BDNF is required for memory of learned fear but not extinction or innate fear. Proc Natl Acad Sci U S A. 2010; 107:2675–2680. [PubMed: 20133801]
35. Liang J, et al. Conditional neuroligin-2 knockout in adult medial prefrontal cortex links chronic changes in synaptic inhibition to cognitive impairments. Mol Psychiatry. 2015
36. Yizhar O, et al. Neocortical excitation/inhibition balance in information processing and social dysfunction. Nature. 2011; 477:171–178. [PubMed: 21796121]
37. Rosas-Vidal LE, Do-Monte FH, Sotres-Bayon F, Quirk GJ. Hippocampal--prefrontal BDNF and memory for fear extinction. Neuropsychopharmacology. 2014; 39:2161–2169. [PubMed: 24625752]
38. Miller EK, Cohen JD. An integrative theory of prefrontal cortex function. Annu Rev Neurosci. 2001; 24:167–202. [PubMed: 11283309]
39. Baldi E, Bucherelli C. Brain sites involved in fear memory reconsolidation and extinction of rodents. Neurosci Biobehav Rev. 2015
40. Marquis JP, Killcross S, Haddon JE. Inactivation of the prelimbic, but not infralimbic, prefrontal cortex impairs the contextual control of response conflict in rats. Eur J Neurosci. 2007; 25:559–566. [PubMed: 17284198]
41. Ragozzino ME. The contribution of the medial prefrontal cortex, orbitofrontal cortex, and dorsomedial striatum to behavioral flexibility. Ann N Y Acad Sci. 2007; 1121:355–375. [PubMed: 17698989]

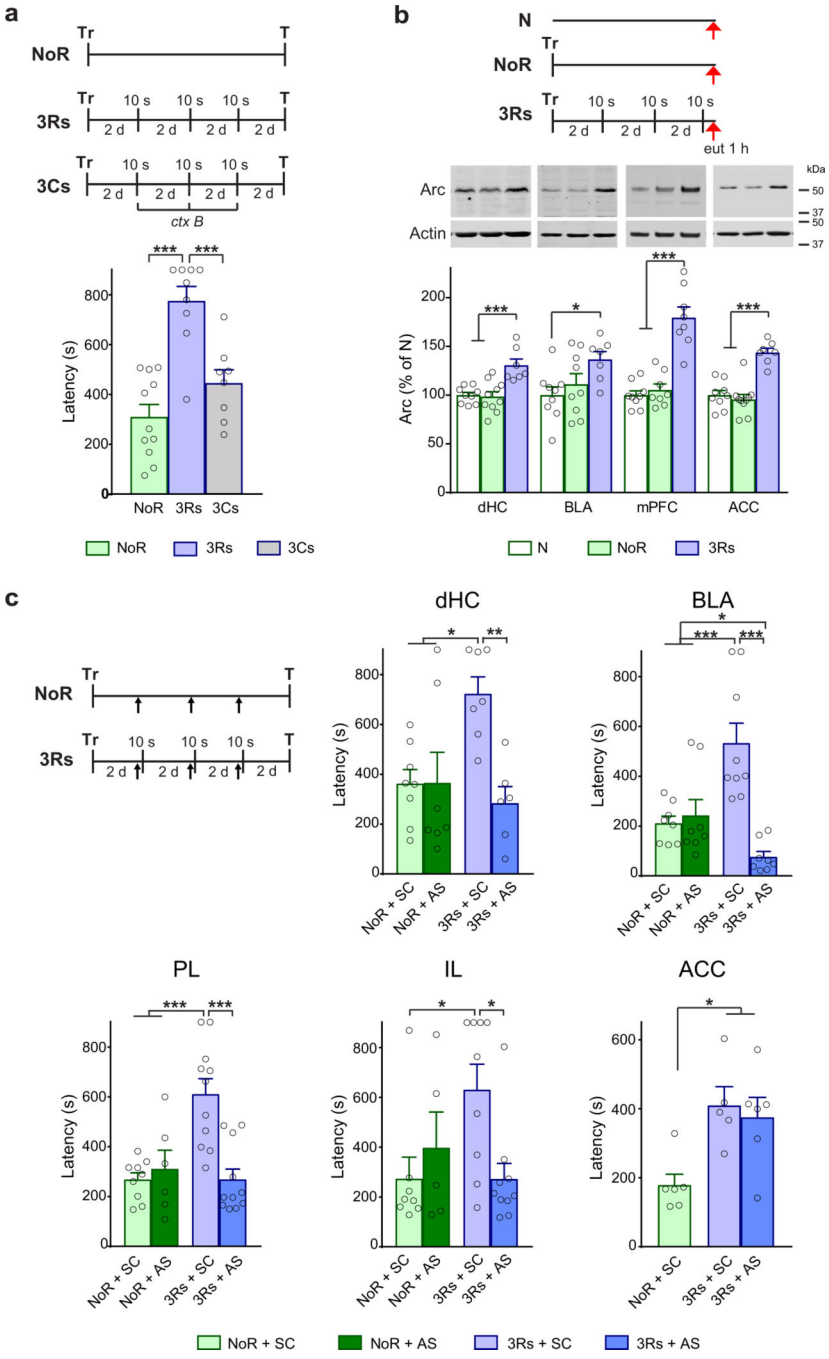

Figure 1. Arc in the dHC and mPFC is required for memory enhancement

(**a**) Mean latency ± s.e.m. of rats trained (Tr), and re-exposed 3 times to the training context (3Rs) or to a novel context (ctx B, 3Cs) for 10 s. NoR: non-retrieval, rats trained and kept in the homecage. Memory retention was tested (T) at 8 d after training (one-way ANOVA followed by Newman-Keuls *post hoc* test, $F_{2, 25} = 20.3$, $P < 0.0001$, n = 11, 9, 8; 3 independent experiments). (**b**) Cropped examples and relative quantitative western blot analyses of dHC, BLA, mPFC and ACC extracts obtained from rats euthanized (eut, red arrows) 1 h after 3Rs, or at matched time point in the NoR group. Naïve rats (N) served as

control. Data are presented as mean percentage ± s.e.m. of the mean values of the N group (one-way ANOVA followed by Newman-Keuls *post hoc* test; dHC $F_{2, 23} = 12.53$, $P = 0.0002$, n = 9, 10, 7; BLA $F_{2, 22} = 3.619$, $P = 0.0438$, n = 9, 9, 7; mPFC $F_{2, 22} = 34.77$, $P < 0.0001$, n = 9, 8, 8; ACC $F_{2, 23} = 26.15$, $P < 0.0001$, n = 9, 10, 7; 3 independent experiments). (**c**) Mean latency ± s.e.m. of rats injected (black arrows) with Arc antisense (AS) or scrambled (SC) oligodeoxynucleotides (ODNs) into the dHC, BLA, PL, IL or ACC 1 h before each 10 s retrieval or at matched time points in the NoR group (one-way ANOVA followed by Newman-Keuls *post hoc* test; dHC $F_{3, 24} = 5.564$, $P = 0.0048$, n = 8, 7, 7, 6; BLA $F_{3, 29} = 12.2$, $P < 0.0001$, n = 8, 8, 9, 8; PL $F_{3, 33} = 11.38$, $P < 0.0001$, n = 9, 6, 11, 11; IL $F_{3, 28} = 3.693$, $P = 0.0234$, n = 8, 5, 9, 10; ACC $F_{2, 14} = 6.565$, $P = 0.0097$, n = 6, 5, 6; 3 independent experiments). Histological images showing the injection sites are presented in Supplementary Figure 10. Full-length blots are presented in Supplementary Figure 11.

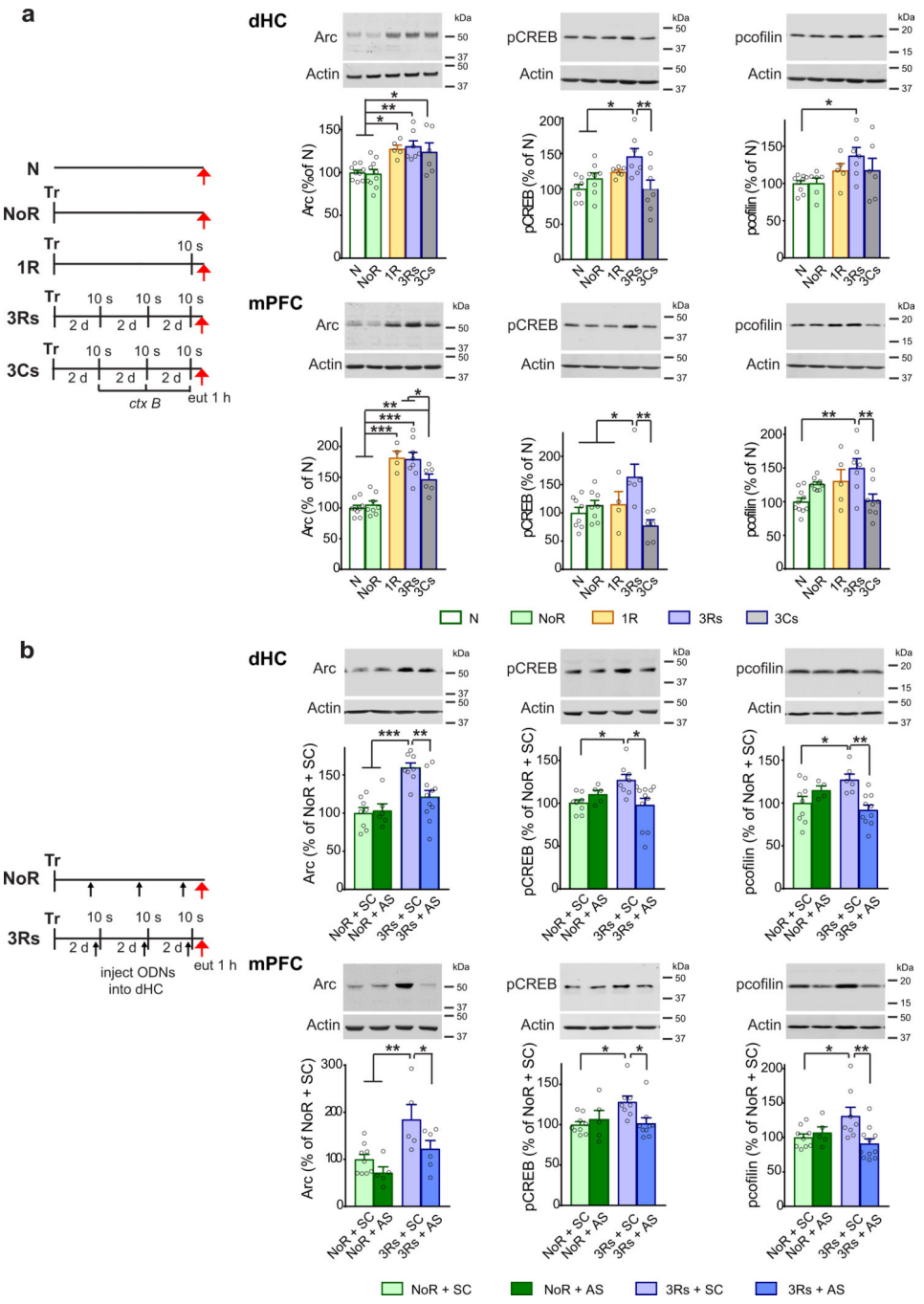

Figure 2. Context retrieval-mediated Arc induction in the dHC controls molecular changes in the mPFC

(**a**) Cropped examples and relative quantitative western blots analyses of dHC and mPFC extracts obtained from rats trained (Tr) and euthanized (eut, red arrows) 1 h after 1 or 3 memory retrievals (1R or 3Rs), or 3 exposures to a novel context (3Cs), or at the matched time point in the non-retrieval (NoR) group. Naïve rats (N) served as reference control. Data are presented as mean percentage ± s.e.m. of the mean values of the N group (one-way ANOVA followed by Newman-Keuls *post hoc* test; dHC: Arc $F_{4, 32} = 7.25$, $P = 0.0003$, n =

9, 10, 5, 7, 6; pCREB $F_{4, 30} = 4.444$, $P = 0.0061$, n = 7, 8, 6, 7, 7; pcofilin $F_{4, 28} = 2.757$, $P = 0.0474$, n = 9, 6, 5, 7, 6; mPFC: Arc $F_{4, 30} = 23.31$, $P < 0.0001$, n = 9, 8, 4, 8, 6; pCREB $F_{4, 26} = 4.745$, $P = 0.0052$, n = 8, 8, 4, 5, 6; pcofilin $F_{4, 33} = 5.041$, $P = 0.0028$, n = 10, 8, 5, 7, 8; 3 independent experiments). (**b**) Cropped examples and relative quantitative western blot analyses of dHC or mPFC extracts obtained from rats euthanized (eut, red arrows) 1 h after 3Rs or at the matched time point in the NoR group. Rats received a bilateral injection (black arrows) of Arc antisense (AS) or scrambled (SC) oligodeoxynucleotides (ODNs) into dHC 1 h before each retrieval, or at the matched time points in the NoR groups. Data are presented as mean percentage ± s.e.m. of the mean values of the NoR + SC group (one-way ANOVA followed by Newman-Keuls *post hoc* test; dHC: Arc $F_{3, 29} = 9.867$, $P = 0.0001$, n = 8, 6, 8, 11; pCREB $F_{3, 28} = 4.165$, $P = 0.0147$, n = 8, 5, 8, 11; pcofilin $F_{3, 25} = 4.927$, $P = 0.008$, n = 9, 4, 6, 10; mPFC: Arc $F_{3, 21} = 6.173$, $P = 0.0036$, n = 9, 5, 5, 6; pCREB $F_{3, 27} = 3.693$, $P = 0.0239$, n = 9, 5, 8, 9; pcofilin $F_{3, 29} = 4.209$, $P = 0.0137$, n = 9, 5, 8, 11; 3 independent experiments). * $P < 0.05$, ** $P < 0.01$, *** $P < 0.001$. Full-length blots are presented in Supplementary Figure 11.

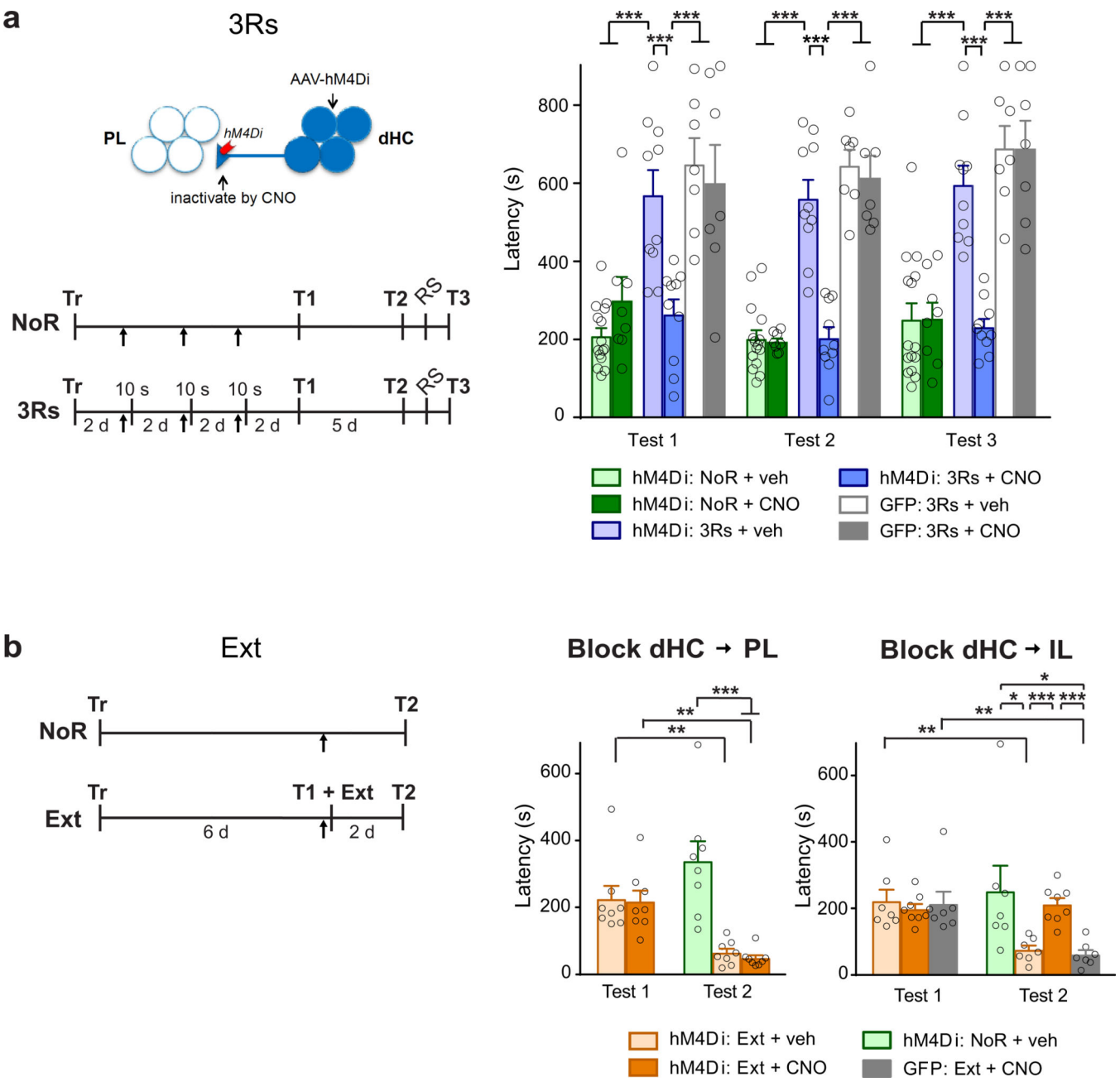

Figure 3. Direct functional dHC-PL projections mediate memory enhancement, but not extinction, which is mediated by dHC-IL projections

(**a**) Cartoon on the top left depicts the strategy for silencing dHC projections into the PL cortex. Mean latency ± s.e.m. of rats infected with AAV8/hSyn-hM4Di-IRES-mCitrine or control AAV8/hSyn-GFP in the dHC, and injected (black arrows) with either CNO or vehicle (veh) into the PL 30 min before each 10 s retrieval (3Rs) or at the matched time points in the NoR group (two-way ANOVA followed by Bonferroni *post hoc* test; treatment $F_{5,\ 153} = 63.67$, $P < 0.0001$; testing $F_{2,\ 153} = 1.59$, $P = 0.2079$; interaction $F_{10,\ 153} = 0.34$, $P = 0.9677$; n = 15, 8, 10, 10, 7, 7; 4 independent experiments). Tr: Training, T1–T3: memory tests; RS: reminder footshock. (**b**) Mean latency ± s.e.m. of rats infected with AAV8/hSyn-

hM4Di-IRES-mCitrine or control AAV8/hSyn-GFP in the dHC, and injected (black arrows) with either CNO or veh into the PL or IL 30 min before extinction (T1 + Ext) or at the matched time points in the NoR group (two-way ANOVA followed by Bonferroni *post hoc* test; block dHC to PL: treatment $F_{1, 28} = 0.19$, $P = 0.6668$; testing $F_{1, 28} = 36.59$, $P < 0.0001$; interaction $F_{1, 28} = 0.03$, $P = 0.8716$; n = 8, 8, 8; block dHC to IL: treatment $F_{2, 38} = 4.73$, $P = 0.0147$; testing $F_{1, 38} = 23.29$, $P < 0.0001$; interaction $F_{2, 38} = 7.99$, $P = 0.0013$; n = 7, 7, 8, 7; 3 independent experiments). Tr: Training, T1–T2: memory tests. * $P < 0.05$, ** $P < 0.01$, *** $P < 0.001$. Histological images showing the injection sites are presented in Supplementary Figure 10.

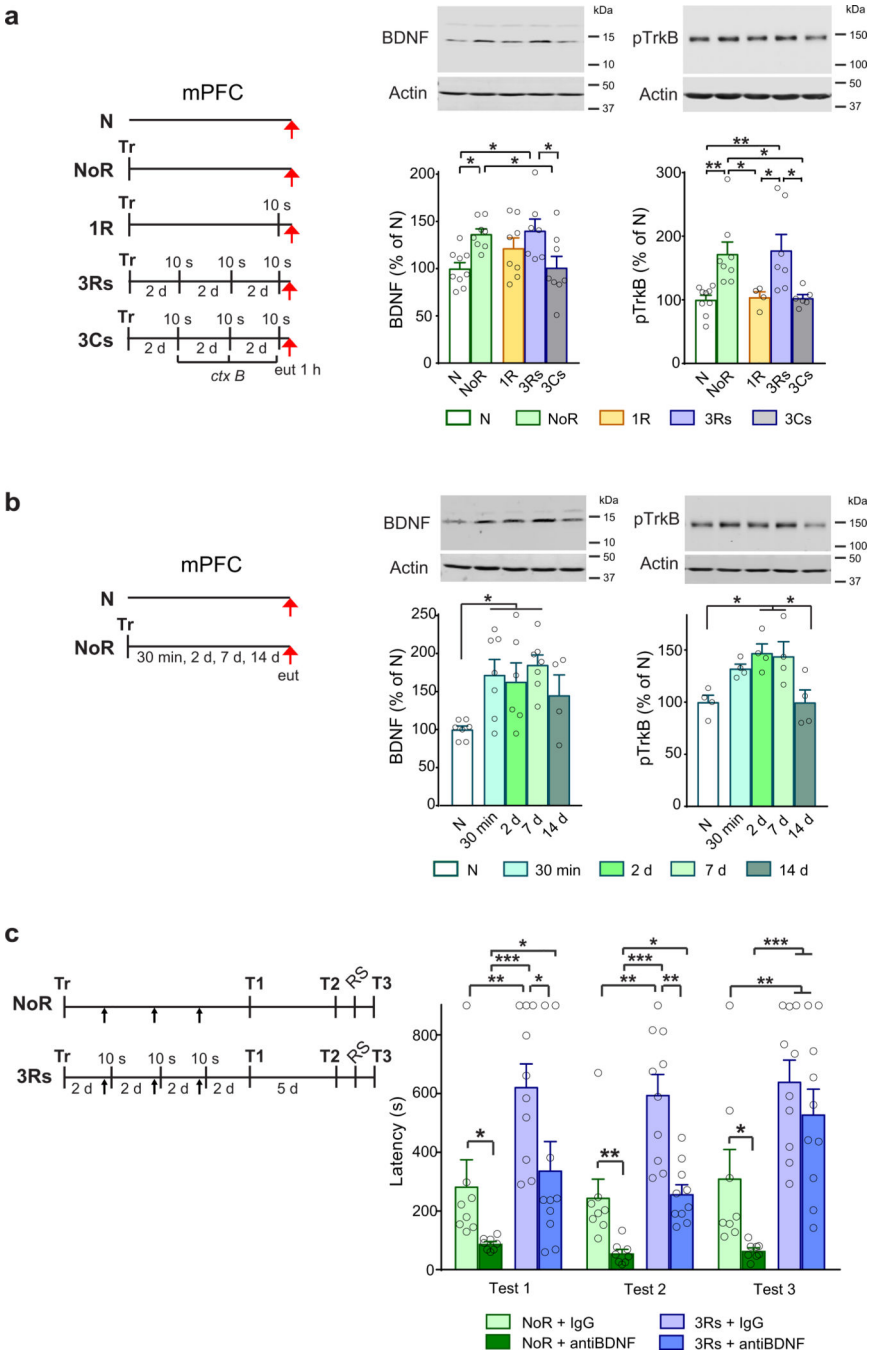

Figure 4. PL BDNF is recruited in IA memory consolidation, and context retrieval-mediated memory enhancement by inhibiting extinction

(**a**) Cropped examples and relative quantitative western blots analyses of mPFC extracts obtained from rats trained (Tr) and euthanized (eut, red arrows) 1 h after 1 or 3 memory retrievals (1R or 3Rs), or 3 exposures to a novel context (3Cs), or at the matched time point in the non-retrieval (NoR) group. Naïve rats (N) served as reference control. Data are presented as mean percentage ± s.e.m. of the mean values of the N group (one-way ANOVA followed by Newman-Keuls *post hoc* test; BDNF $F_{4, 35} = 3.942$, $P = 0.0096$, n = 9, 8, 8, 7, 8;

pTrkB $F_{4, 29} = 6.307$, $P = 0.0009$, n = 9, 8, 4, 7, 6; 3 independent experiments). (**b**) Cropped examples and relative quantitative western blots analyses of mPFC extracts obtained from rats euthanized (eut, red arrows) at 30 min, 2 d, 7 d and 14 d after IA training (Tr). Naïve rats (N) served as reference control. Data are presented as mean percentage ± s.e.m. of the mean values of the N group (one-way ANOVA followed by Newman-Keuls *post hoc* test; BDNF $F_{4, 26} = 3.722$, $P = 0.0159$, n = 7, 7, 6, 7, 4; pTrkB $F_{4, 15} = 5.646$, $P = 0.0056$, n = 4, 4, 4, 4, 4; 2 independent experiments). (**c**) Mean latency ± s.e.m. of rats trained (Tr) and received 3 context reactivations (3Rs) or left in the homecage (NoR), tested as shown in the schema (T1–T3) and -where indicated - exposed to a reminder footshock (RS). AntiBDNF blocking antibody or control IgG was injected (black arrows) into PL cortex 30 min before each 10 s retrieval or at the matched time points for the NoR group (two-way ANOVA followed by Bonferroni *post hoc* test; treatment $F_{3, 96} = 31.3$, $P < 0.0001$; testing $F_{2, 96} = 1.89$, $P = 0.1561$; interaction $F_{6, 96} = 0.83$, $P = 0.5476$; n = 8, 8, 10, 10; 3 independent experiments). * $P < 0.05$, ** $P < 0.01$, *** $P < 0.001$. Histological images showing the injection sites are presented in Supplementary Figure 10. Full-length blots are presented in Supplementary Figure 12.

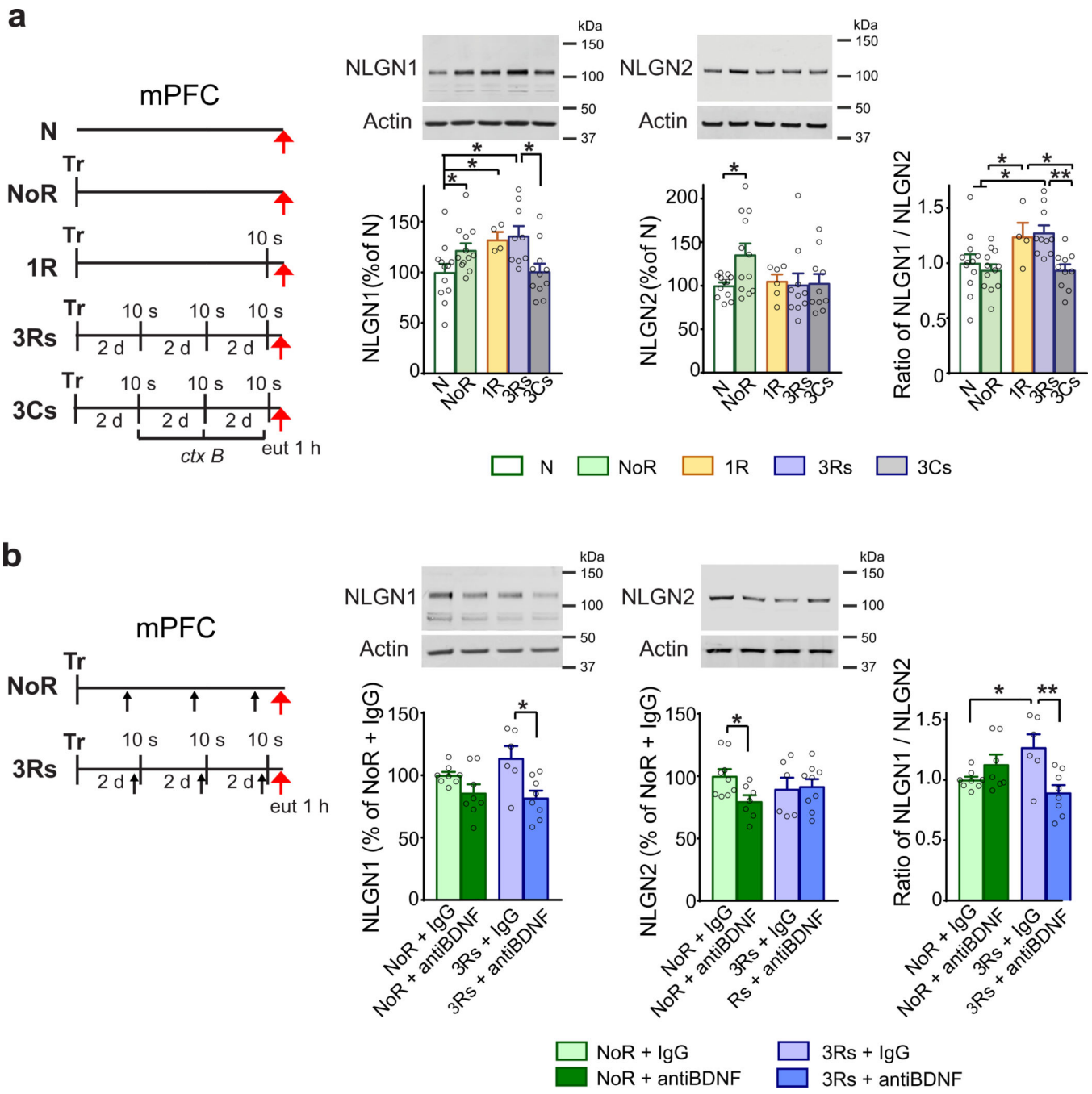

Figure 5. PL BDNF regulates NLGN1/NLGN2 ratio in memory consolidation and retrieval-dependent memory enhancement

(**a**) Cropped examples and relative quantitative western blots analyses of mPFC extracts obtained from rats trained (Tr) and euthanized (eut, red arrows) 1 h after 1 or 3 memory retrievals (1R or 3Rs), or 3 exposures to a novel context (3Cs), or at the matched time point in the non-retrieval (NoR) group. Naïve rats (N) served as reference control. Data are presented as mean percentage ± s.e.m. of the mean values of the N group (one-way ANOVA followed by Newman-Keuls *post hoc* test; NLGN1 $F_{4, 43} = 4.110$, $P = 0.0066$, n = 12, 12, 4, 9, 11; NLGN2 $F_{4, 45} = 2.285$, $P = 0.0749$, n = 12, 12, 6, 10, 10; 3 independent experiments).

Right panel: the ratio of NLGN1/NLGN2 shown as mean ± s.e.m. relative to the mean value of the N group (one-way ANOVA followed by Newman-Keuls *post hoc* test; $F_{4, 42} = 4.825$, $P = 0.0027$, n = 12, 12, 4, 9, 10; 3 independent experiments). (**b**) Cropped examples and relative quantitative western blot analyses of mPFC extracts obtained 1 h after 3Rs or at the matched time point in the NoR group. AntiBDNF or control IgG antibody was injected (black arrows) into PL 30 min before each 10 s retrieval or at the match time points in the NoR group. Data are presented as mean percentage ± s.e.m. of the mean values of the NoR + IgG group (one-way ANOVA followed by Newman-Keuls *post hoc* test; NLGN1 $F_{3, 26} = 4.737$, $P = 0.0091$, n = 8, 8, 6, 8; NLGN2 $F_{3, 27} = 1.757$, $P = 0.1792$, n = 9, 7, 6, 9; 3 independent experiments). Right panel: The ratio of NLGN1/NLGN2 shown as mean ± s.e.m. relative to the mean value of the NoR + IgG group (one-way ANOVA followed by Newman-Keuls *post hoc* test; $F_{3, 25} = 4.999$, $P = 0.0075$, n = 8, 7, 6, 8; 3 independent experiments). * $P < 0.05$, ** $P < 0.01$. Full-length blots are presented in Supplementary Figure 12.

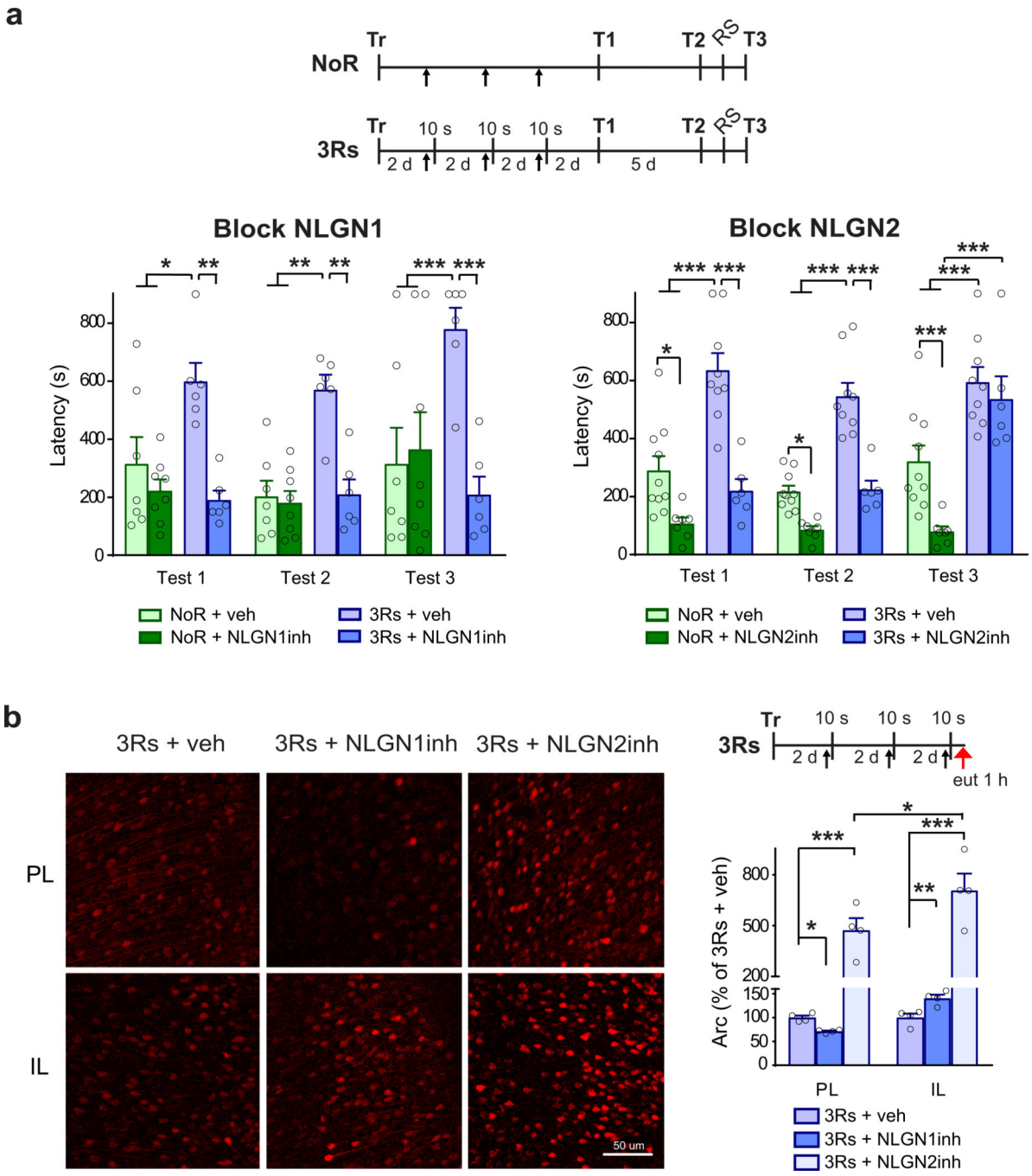

Figure 6. NLGN1 and NLGN2 have distinct roles in memory strengthening and extinction suppression

(**a**) Mean latency ± s.e.m. of rats trained (Tr) and received 3 memory retrievals (3Rs) or left in the homecage without retrieval (NoR) after training (Tr), tested as shown in the schema (T1–T3) and exposed to a reminder footshock (RS) where indicated. NLGN1 or NLGN2 function was blocked with recombinant extracellular domain of NLGN1 or NLGN2 (NLGN1inh or NLGN2inh) injected (black arrows) into PL 30 min before each 10 s retrieval or at the matched time points in the NoR group (two-way ANOVA followed by Bonferroni

post hoc test; block NLGN1: treatment $F_{3, 69} = 18.84$, $P < 0.0001$; testing $F_{2, 69} = 2.69$, $P = 0.0752$; interaction $F_{6, 69} = 0.52$, $P = 0.7924$; n = 7, 8, 6, 6; block NLGN2: treatment $F_{3, 84} = 61.46$, $P < 0.0001$; testing $F_{2, 84} = 6.03$, $P = 0.0036$; interaction $F_{6, 84} = 3.13$, $P = 0.0081$; n = 10, 7, 9, 6; 3 independent experiments). (**b**) Examples and quantification of immunofluorescent staining of Arc in the PL and IL obtained from rats euthanized (eut, red arrow) 1 h after 3Rs from the rats injected (black arrows) with control vehicle (veh), NLGN1inh or NLGN2inh into PL. Data are presented as mean percentage ± s.e.m. of the mean values of the 3Rs + veh group (two-way ANOVA followed by Bonferroni *post hoc* test; treatment $F_{2, 18} = 63.02$, $P < 0.0001$; region $F_{1, 18} = 6.25$, $P = 0.0223$; interaction $F_{2, 18} = 2.95$, $P = 0.0777$; n = 4, 4, 4; 2 independent experiments). * $P < 0.05$, ** $P < 0.01$, *** $P < 0.001$. Histological images showing the injection sites are presented in Supplementary Figure 10.

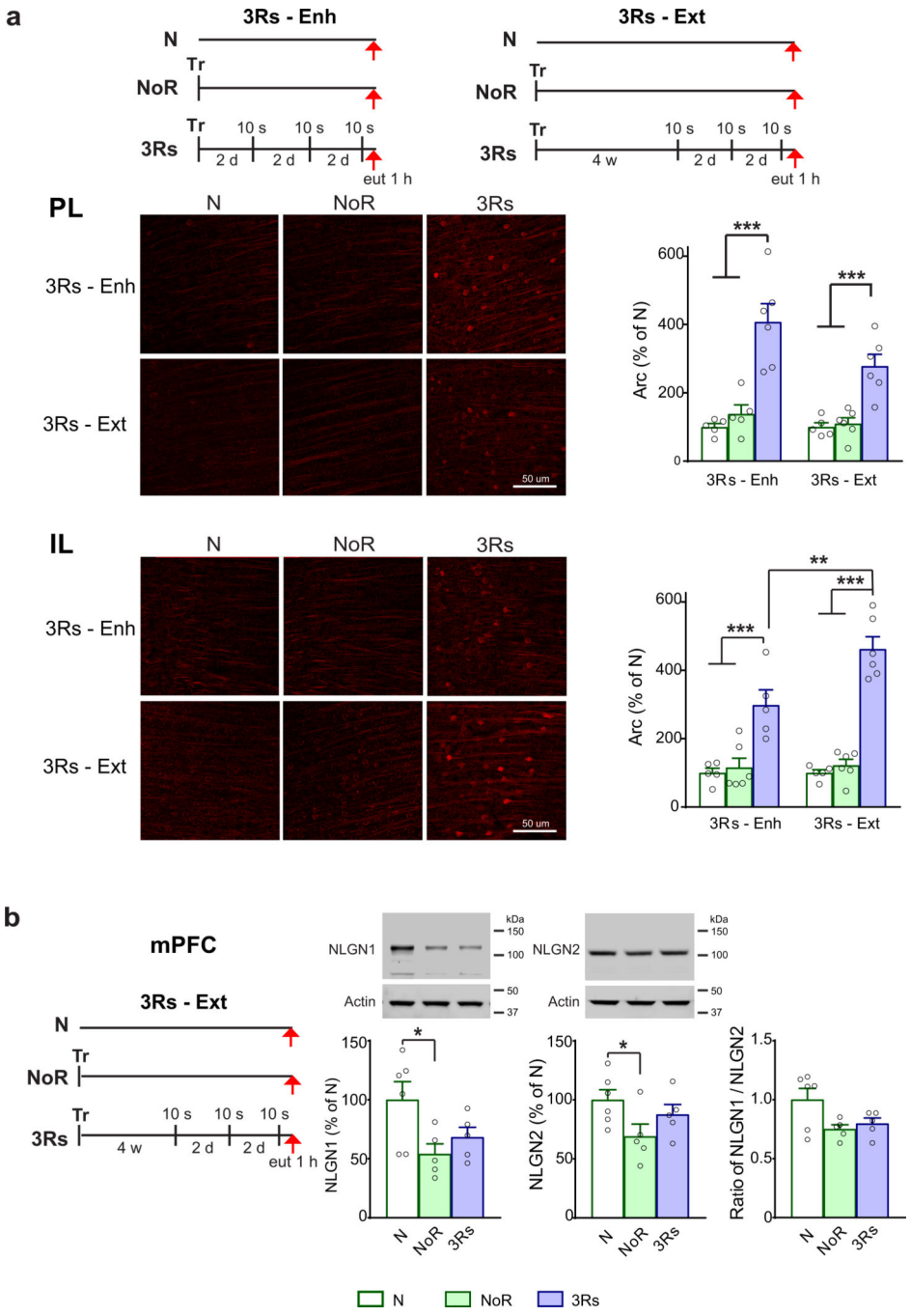

Figure 7. Changes in NLGN1 and NLGN2 in the mPFC correlate with retrieval-mediated memory strengthening or extinction

(**a**) The schemas of the experimental paradigms are shown on the top. Examples and quantification of immunofluorescence staining of Arc in the PL and IL from rats trained (Tr) and euthanized (eut, red arrows) 1 h after 3Rs starting 2 days (enhancement paradigm, 3Rs - enh; n = 5, 5, 6) *vs.* 4 weeks (extinction paradigm, 3Rs - ext; n = 5, 6, 6) post-training, or in the matching naïve (N) and non-retrieval (NoR) groups. Data are presented as mean percentage ± s.e.m. of the mean values of the N group (two-way ANOVA followed by

Bonferroni *post hoc* test; PL: treatment $F_{2, 27} = 36.98$, $P < 0.0001$; time $F_{1, 27} = 4.06$, $P = 0.0538$; interaction $F_{2, 27} = 2.35$, $P = 0.1145$; IL: treatment $F_{2, 27} = 62.13$, $P < 0.0001$; time $F_{1, 27} = 6.16$, $P = 0.0196$; interaction: $F_{2, 27} = 5.47$, $P = 0.0101$; 2 independent experiments). (**b**) Cropped examples and relative quantitative western blot analyses of mPFC extracts obtained from rats euthanized (eut, red arrows) 1 h after 3Rs - ext or at the matched time point in the NoR group. Naïve rats (N) served as reference control. Data are presented as mean percentage ± s.e.m. of the mean values of the N group. The ratio of NLGN1/NLGN2 is shown as mean ± s.e.m. relative to the mean value of the N group (one-way ANOVA followed by Newman-Keuls *post hoc* test; NLGN1 $F_{2, 13} = 4.011$, $P = 0.0440$, n = 6, 5, 5; NLGN2 $F_{2, 13} = 2.908$, $P = 0.0904$, n = 6, 5, 5; ratio of NLGN1/NLGN2: $F_{2, 13} = 3.715$, $P = 0.0530$, n = 6, 5, 5; 2 independent experiments). * $P < 0.05$, ** $P < 0.01$, *** $P < 0.001$. Full-length blots are presented in Supplementary Figure 12.

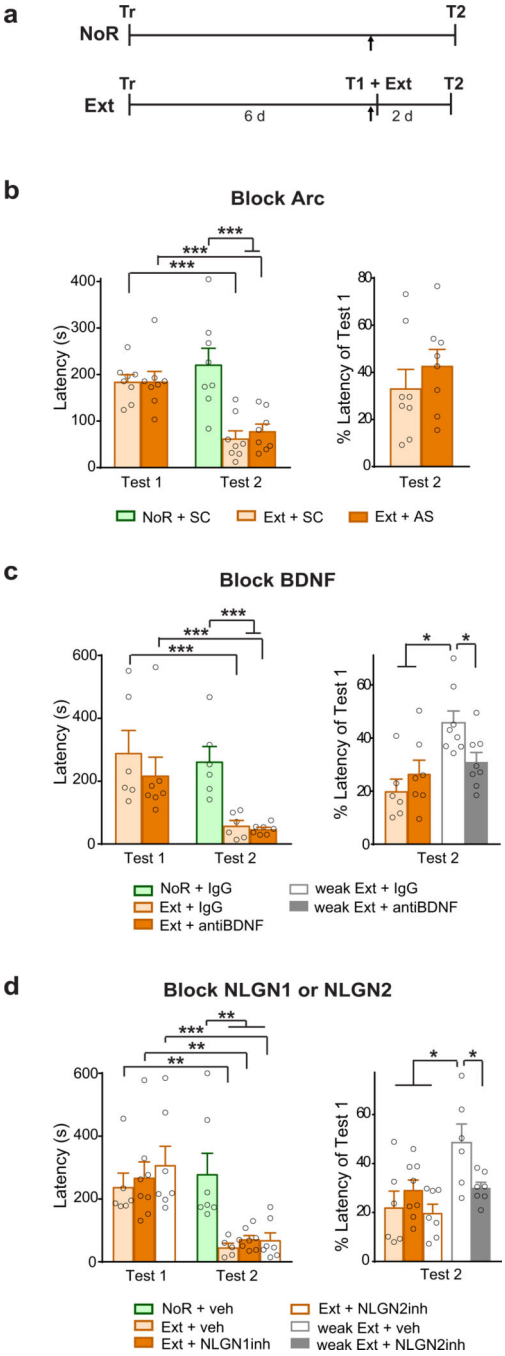

Figure 8. PL Arc, BDNF, NLGN1 and NLGN2 are not required for extinction. PL BDNF and NLGN2 suppress extinction

(**a**) The schemas of the experimental paradigms. Tr: Training, T1–T2: memory tests; Ext: extinction; black arrows: injections into PL cortex (**b**) Mean latency ± s.e.m. of rats injected with Arc antisense (AS) or scrambled (SC) oligodeoxynucleotides (ODNs) 1 h before T1 + Ext or at the matched time point in the NoR group (two-way ANOVA followed by Bonferroni *post hoc* test; treatment $F_{1, 24} = 0.57$, $P = 0.4568$; testing $F_{1, 24} = 30.15$, $P < 0.0001$; interaction $F_{1, 24} = 0.65$, $P = 0.4285$; n = 8, 8, 6; 3 independent experiments). Panel

on the right shows the latency at test 2 presented as mean ± s.e.m. of the mean latency at test 1, for the extinction (Ext) groups (unpaired two-tailed Student *t*-test; $t_{14} = 0.0922$, $P = 0.3822$; n = 8, 6). (**c**) Mean latency ± s.e.m. of rats injected with antiBDNF blocking antibody or its control IgG 30 min before T1 + Ext (two-way ANOVA followed by Bonferroni *post hoc* test; treatment $F_{1, 22} = 0.81$, $P = 0.3781$; testing $F_{1, 22} = 18.71$, $P = 0.0003$; interaction $F_{1, 22} = 0.43$, $P = 0.5201$; n = 6, 6, 7; 3 independent experiments). Panel on the right shows the latency at test 2 presented as mean ± s.e.m. of the mean latency at test 1, for both the extinction (Ext) groups and the weak extinction (weak Ext) groups (one-way ANOVA followed by Newman-Keuls *post hoc* test; $F_{3, 25} = 6.104$, $P = 0.0029$, n = 6, 7, 8, 8). (**d**) Mean latency ± s.e.m. of rats injected with inhibitors of NLGN1 (NLGN1inh) or NLGN2 (NLGN2inh) or their vehicle (veh) 30 min before T1 + Ext (two-way ANOVA followed by Bonferroni *post hoc* test; treatment $F_{2, 36} = 0.65$, $P = 0.5259$; testing $F_{1, 36} = 42.29$, $P < 0.0001$; interaction $F_{2, 36} = 0.22$, $P = 0.8069$; n = 7, 6, 8, 7; 3 independent experiments). Panel on the right shows the latency at test 2 presented as mean ± s.e.m. of the mean latency at test 1, for both the extinction (Ext) groups and the weak extinction (weak Ext) groups (one-way ANOVA followed by Newman-Keuls *post hoc* test; $F_{4, 29} = 4.833$, $P = 0.0041$, n = 6, 8, 7, 6, 7). * $P < 0.05$, ** $P < 0.01$, *** $P < 0.001$. Histological images showing the injection sites are presented in Supplementary Figure 10.